Piezoelectric ZnO Thin Films for 2DOF MEMS Vibrational Energy Harvesting

Kai Tao[1], Haiping Yi[1], Lihua Tang[2], Jin Wu[3], Liangxing Hu[4], Nan Wang[4], Richad Fu[5], Jianmin Miao[4] and Honglong Chang[1]

[1]Ministry of Education Key Laboratory of Micro and Nano Systems for Aerospace, Northwestern Polytechnical University, Xi'an 710072, PR China

[2]Department of Mechanical Engineering, University of Auckland, 20 Symonds Street, Auckland 1010, New Zealand

[3]State Key Laboratory of Optoelectronic Materials and Technologies, School of Electronics and Information Technology, Sun Yat-sen University, Guangzhou 510275, PR China

[4]School of Mechanical and Aerospace Engineering, Nanyang Technological University, 50 Nanyang Avenue, 639798 Singapore

[5]Faculty of Engineering and Environment, University of Northumbria, Newcastle upon Tyne NE1 8ST, UK

Abstract. Zinc oxide (ZnO) as an environmental-friendly non-ferroelectric material plays an essential role in microelectromechanical systems (MEMS) due to its excellent semiconducting and piezoelectric properties. For the first time, a fully integrated two-degree-of-freedom (2DOF) MEMS piezoelectric vibration energy harvester (p-VEH) using ZnO thin films has been presented for converting ambient kinetic energy to electrical energy. The 2DOF energy harvesting system comprises of two subsystems: the primary subsystem for energy conversion and the auxiliary subsystem for frequency adjustment. Piezoelectric ZnO thin film is deposited on the primary subsystem for strain-to-electricity energy conversion through room-temperature RF magnetron sputtering method. The dynamic behavior of proposed 2DOF resonant system is examined and optimized by a lumped parametric numerical model. Two close and comparable peaks are found to be likely achieved by carefully adjusting mass and frequency ratios. The MEMS energy harvesting chip has been fabricated through a laminated surface micromachining with double-side bulk micromachining process. The surface morphology and crystalline quality of ZnO-based MEMS device is characterized through field-emission scanning electron microscopy (FE-SEM), and energy-dispersive X-ray spectroscopy (EDS), respectively. With the fabricated prototype excited at 0.5 g, two close peaks of 403.8 and 489.9 Hz with comparable voltages of 10 and 15 mV are obtained, providing good agreement with the modeling predictions.

Submitted to: *Surface & Coatings Technology*

1. Introduction

Recent advances in internet of things (IoT) and wireless sensor networks reveal new insight into sustainability and availability of new type micro energy storage and conversion devices, including MEMS-based micro/nano generators, themoelectrics and solar cells. Typical MEMS-based vibration energy harvesters are capable of transforming mechanical energy to electrical energy through piezoelectric [1-3], electromagnetic [4-6], electrostatic [7-9] and triboelectric mechanisms [10-12]. Piezoelectric materials possess the unique merit of direct electromechanical coupling that can convert mechanical strain to electrical energy and vice versa. MEMS piezoelectric vibration energy harvesters (p-VEH) have the merits of high power density and ease of miniaturization. Therefore, MEMS p-VEH is capable of converting kinetic energy to electrical energy by continuously pre-stressing or stretching piezoelectric materials under external cycling excitations.

Generally, the performance of p-VEHs is highly dependent on the piezoelectric properties of the materials. The piezoelectric materials can be categorized into several forms, including piezoceramic (PZT or lead zirconate titanate), Barium titanate ($BaTiO_3$), single crystal (quartz), thin film (ZnO or AlN), thick film based on piezoceramic powder and polymeric materials (PVDF). Although piezoceramics including PZT and Micro-Fiber-Composites (MFC) are most commonly used piezoelectric materials in traditional energy harvesting applications, they encounter difficulties in miniaturization and thin film depositions in MEMS fabrication process [13]. These make them not feasible in micro-scale applications. ZnO is an environmental-friendly non-ferroelectric material and has excellent semiconducting and piezoelectric properties[14]. Compared to the AlN-based piezoelectric film deposition process, the formation of ZnO piezoelectric thin film does not require high-temperature annealing process or high-voltage poling process. Due to these unique merits, ZnO-based piezoelectric thin film plays an essential role in microelectromechanical systems (MEMS), such as sensors [15], actuators [16] , acoustic wave generations [17] and smart slider to detect the head-disk contact [18]. In the current study, we are endeavor to applying ZnO-based piezoelectric thin film to a fully integrated MEMS p-VEH for converting ambient kinetic energy to electrical energy.

Regarding to vibration-based MEMS energy harvesting applications, one of the key challenges is the narrow bandwidth problem [19]. The MEMS-based energy harvester is usually designed as single spring-mass-damper system. The kinetic energy can only be scavenged near its sole resonance while the ambient vibrations usually have broadband frequency spectrums. To address these limitations, numerous frequency broadening approaches have been proposed, categorized as multimodal energy harvesting [20-22], resonance tuning [23] and nonlinear technique [24-26]. For MEMS-based p-VEH energy harvesters, multimodal techniques are more advantageous in terms of wafer-level fabrication and rare post-assembly process.

In the current work, for the first time, we presented a ZnO-based MEMS p-VEH with two-degree-of-freedom (2DOF) multimodal system. The 2DOF multimodal system has a primary subsystem for energy conversion and an auxiliary subsystem for frequency adjustment. Piezoelectric ZnO thin film is deposited on the primary subsystem for strain-to-electricity energy conversion. The details of device design, fabrication and characterization will be deliberated in the following sections.

2. Device Design and Fabrication

The schematic design of 2DOF MEMS vibrational energy harvester with piezoelectric ZnO thin films is shown in Figure 1. The device consists mainly of two parts, the 2DOF spring-mass resonant structure and ZnO-based piezoelectric thin film.

The 2DOF resonant structure is constructed on a $SiO_2/Si/SiO_2$ wafer. It is composed of two subsystems, the inner auxiliary frequency tuning system and the outer primary power generation system. The inner auxiliary subsystem has a circular mass suspended by three parallel spiral beams around. The diameter and height of the circular mass is 3.4 mm and 500 μm, respectively. The geometry of spiral beam is formed with three 120° circular arcs, which are designed with different radii and tangent connected to each other at the conjunction points. The outer primary subsystem has a ring shape mass suspended by three small arc beams. The ring shape mass has 5.4 mm outer radius, 2.05 mm inner radius and 500 μm height. Each small arc beam is 5.75 mm in outer radius, 5.5 mm in inner radius and 45 μm in height. The arc beams are evenly arranged in rotatory symmetry with 120°distributed around the primary mass. It is worth noting that the heights of both the outer and inner masses are the same as the wafer thickness of 500 μm, while the suspended beams are only 45 μm in height formed by double-side deep reactive ion etching (DRIE) process. The low stiffness and large mass congfiguration will facilitate to achieve low resonance of the whole 2DOF system.

The piezoelectric ZnO thin film is patterned on the top of the outer arc beams for energy conversion, as shown in Figure 1. The ZnO thin film is sandwiched with top and bottom Pt/Au electrode layers. Since ZnO is non-ferroelectric materials, the whole process is conducted in the room temperature environment, making high-temperature post annealing or high-voltage poling process not necessary. When an external vibration excites the 2DOF spring-mass resonant structure, the ZnO thin film on the surface of outer arc beams would suffer continuously prestressing and stretching, resulting mechanical energy to electrical energy conversion.

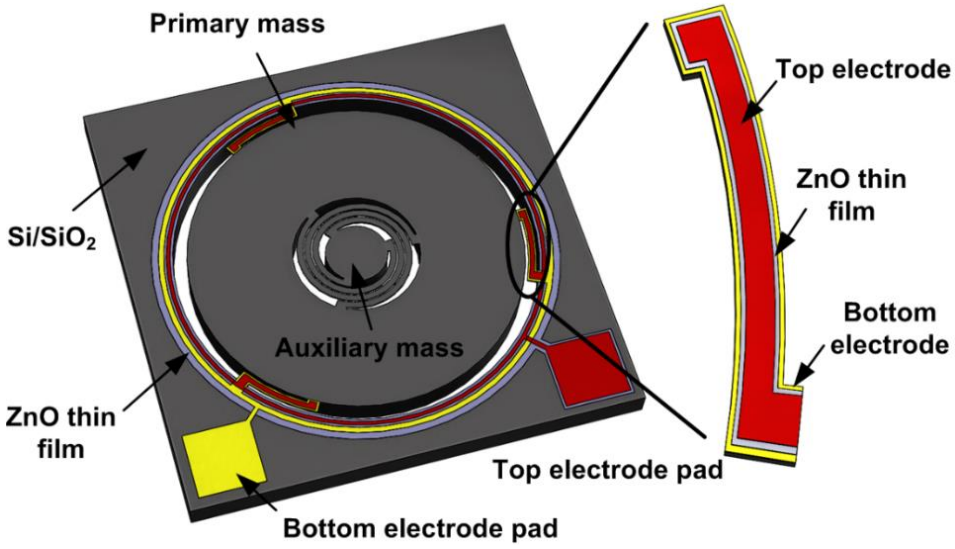

Figure 1. *Schematic of 2DOF MEMS vibrational energy harvesting chip with piezoelectric ZnO thin films and enlarged view of top electrode layer/ZnO layer/bottom electrode layer sandwiched structure*

The fabrication flow of ZnO-based 2DOF MEMS energy harvesting chip is depicted in Figure 2. The process includes sacrificial layer-by-layer surface micromachining process and double-side DRIE bulk micromachining process. It begins with a 500 μm thick SiO_2/Si/SiO_2 wafer substrate. Pt (150nm)/Au (150nm) conducting layer is patterned on the top of SiO_2 insulation layer through a sputtering and lift-off process (figure 2(a)). The Pt/Au layer serves as bottom electrode. Photoresist is then spin coated on the surface of bottom electrode. This is followed by lithography process to create openings for next thin film deposition (figure 2(b)). One of the critical processes is the room-temperature deposition of ZnO piezoelectric thin film from a 3 mm thick and 99.99% purity ZnO target in the RF magnetron sputtering system (figure 2(c)). After that, the surplus ZnO is removed by wet etching process (figure 2(d)). Repeatedly, another Pt (150nm)/Au (150nm) layer served as top electrode is deposited on the top of ZnO layer through the same lift-off process as shown in Figure 2(b). Thus, the top electrode layer/ZnO layer/bottom electrode layer is formed with a sandwiched structure (figure 2(e)). After the piezoelectric thin film deposition is finished, the next step is to define the 2DOF resonant structure. SiO_2 opening via is formed by photolithography and reactive-ion etching (RIE) process (figure 2(f)). Subsequently, DRIE process is applied to etch away the silicon substrate to pattern the front-side spring-mass structure (figure 2(g)). The wafer is front-side bonded to another supporting wafer with heat conductive silver paste and then flipped over with backside DRIE process to form the seismic mass. Finally, the supporting wafer is removed and the whole ZnO-based 2DOF MEMS energy harvesting chip is released (figure 2(f)).

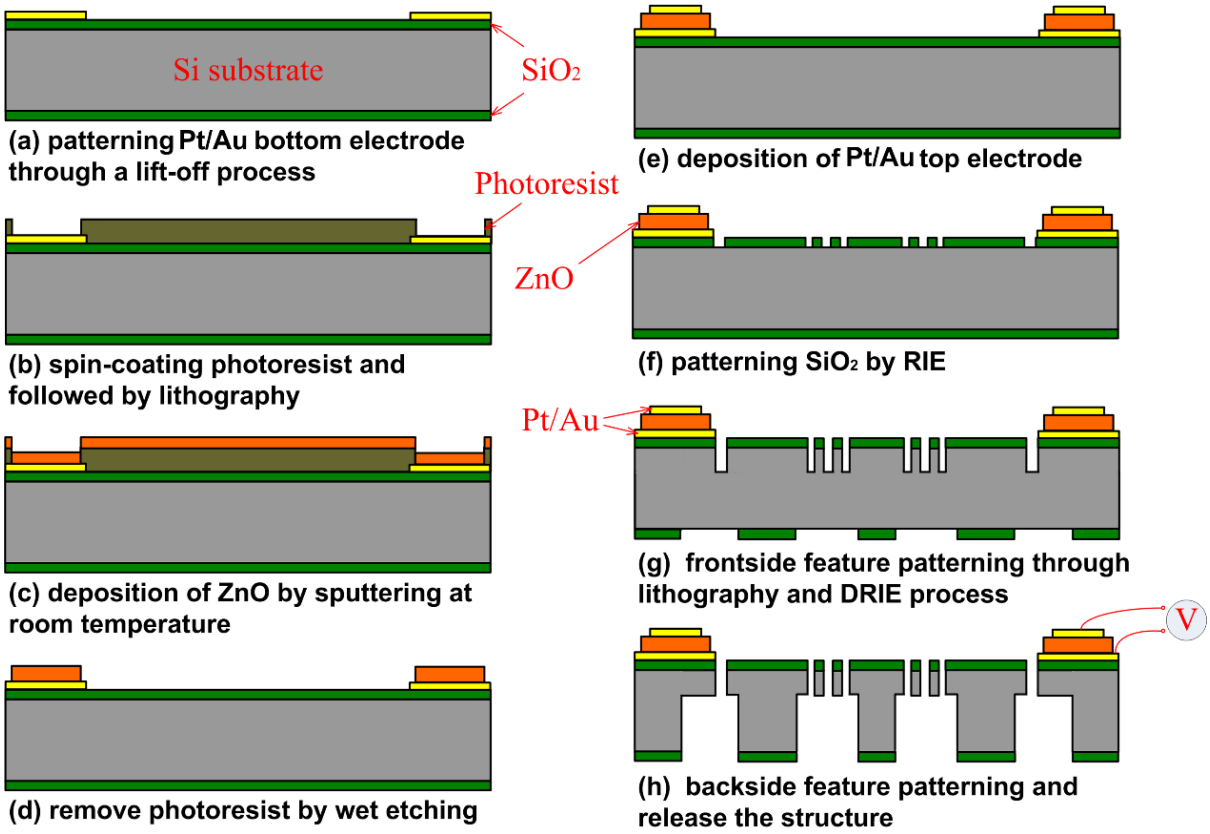

Figure 2. *Fabrication flow of ZnO-based 2DOF MEMS energy harvesting chip on SiO_2/Si/ SiO_2 wafers*

3. Parametric Analysis of Piezoelectric 2DOF System

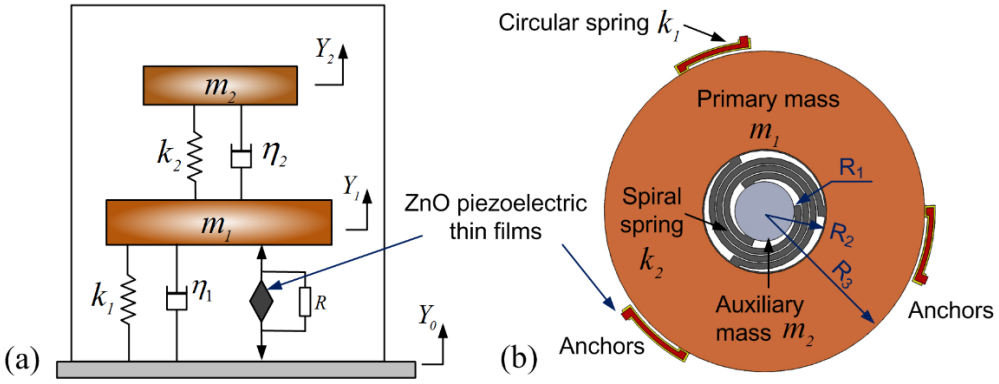

Figure 3. *Lumped parameter model of proposed 2DOF p-VEH with ZnO piezoelectric thin films;(b) the corresponding 2DOF spring-mass resonant structure*

The lumped parametric model of proposed 2DOF p-VEH and the corresponding spring-mass resonant structure are shown in Figure 3(a) and 3(b), respectively. In the current study, the energy harvesting resonant system is designed with two-degree-of-freedom structures aiming to achieve two close and comparable peaks. These enable the proposed harvester to be more adaptive to some practical kinetic scenarios where the vibration sources may has multiple peaks. The 2DOF p-VEH resonant system is composed of a primary subsystem and an auxiliary subsystem. The primary subsystem has primary mass m_1, mechanical damping η_1, spring stiffness k_1 and piezoelectric energy conversion element. The auxiliary subsystem has the auxiliary mass m_2, mechanical damping η_2 and spring stiffnessk_2. According to the lumped parametric model shown in Figure 3(a), the governing equation of 2DOF piezoelectric energy conversion system can be derived as

$$\begin{cases} m_1\left(\ddot{Y}_1-\ddot{Y}_0\right)+\eta_1\left(\dot{Y}_1-\dot{Y}_0\right)+k_1\left(Y_1-Y_0\right)+\theta V-\eta_2\left(\dot{Y}_2-\dot{Y}_1\right)-k_2\left(Y_2-Y_1\right)=-m_1\ddot{Y}_0 \\ m_2\left(\ddot{Y}_2-\ddot{Y}_1\right)+\eta_2\left(\dot{Y}_2-\dot{Y}_1\right)+k_2\left(Y_2-Y_1\right)=-m_2\ddot{Y}_1+m_2\ddot{Y}_0-m_2\ddot{Y}_0 \end{cases} \tag{1}$$

where θ is the piezoelectric electromechanical coupling coefficient, V is the voltage across the resistance R, θV is the backward electromechanical coupling force (θV) induced by piezoelectric ZnO thin film. Considering the weak coupling conditions in the current energy conversion system, the effect of the backward electromechanical coupling force (θV) on the dynamic behavior of the 2DOF resonant system is negligible. Therefore, by letting $x=Y_1-Y_0$ and $y=Y_2-Y_1$, the equation (1) can be represented as

$$\begin{cases} \left(m_1+m_2\right)\ddot{x}+\eta_1\dot{x}+k_1x+m_2\ddot{y}=-\left(m_1+m_2\right)\ddot{Y}_0 \\ m_2\ddot{y}+\eta_2\dot{y}+k_2y=-m_2\ddot{x}-m_2\ddot{Y}_0 \end{cases} \tag{2}$$

In order to achieve two close and comparable peaks, the mass ratio (μ) and frequency tuning ratio (α) should be carefully adjusted in the parametric model. Letting

$$\omega_1=\sqrt{\frac{k_1}{m_1}},\quad \omega_2=\sqrt{\frac{k_2}{m_2}},\quad \zeta_1=\frac{\eta_1}{2\sqrt{k_1m_1}},\quad \zeta_2=\frac{\eta_2}{2\sqrt{k_2m_2}},\quad \mu=\frac{m_2}{m_1},\quad \alpha=\frac{\omega_2}{\omega_1},\quad \Omega=\frac{\omega}{\omega_1} \tag{3}$$

Applying Laplace transform and setting $s = j\omega$, the equation (2) can be derived as

$$\begin{cases} (1+\mu)s^2\hat{X} + 2\zeta_1\omega_1 s\hat{X} + \omega_1^2\hat{X} + \mu s^2\hat{Y} = -(1+\mu)s^2\hat{Y} \\ s^2\hat{Y} + 2\zeta_2\omega_2 s\hat{Y} + \omega_2^2\hat{Y} = -s^2\hat{X} - s^2 Y_0 \end{cases} \tag{4}$$

where μ, α and ζ are the dimensionless parameters representing the mass ratio, frequency tuning ratio and the damping ratio, respectively. ω_1 and ω_2 are the resonances of the primary and auxiliary subsystem, respectively. By solving the equation (4), the normalized displacement of the primary mass can be obtained as

$$\left|\tilde{X}\right| = \left| \frac{\Omega^2\left(1+\mu-\dfrac{\Omega^2}{\alpha^2 + j2\zeta_2\alpha\Omega}\right)}{1-(1+\mu)\Omega^2 + j2\zeta_1\Omega + \dfrac{\Omega^4 - \Omega^2 - j2\zeta_1\Omega^3}{\alpha^2 + j2\zeta_2\alpha\Omega}} \right| \tag{5}$$

Figure 4 shows the contour plotting of normalized displacement of the primary mass versus different mass ratios (μ) and frequency tuning ratios (α) under various excitation frequencies (Ω): (a) α=0.8; (b) α=0.9; (c) α=1.0; (d) α=1.1. The primary damping (ζ_1) and the auxiliary damping (ζ_2) are set as the same as 0.004. It can be clearly observed that two peaks can be created with the proposed 2DOF resonant system. When controlling the frequency tuning ratio (α) in 0.9～1 and mass ratio (μ) approximate to 0, two close and comparable peaks can be obtained, as depicted in Figure 4(b-c). In the current study, the frequency tuning ratio (α) and mass ratio (μ) are set as 0.92 and 0.04, respectively. These form a theoretical foundation of the mechanical design of proposed 2DOF spring-mass system. The details of the design parameters of proposed 2DOFpiezoelectric MEMS energy harvesting chip are illustrated in the Table 1.

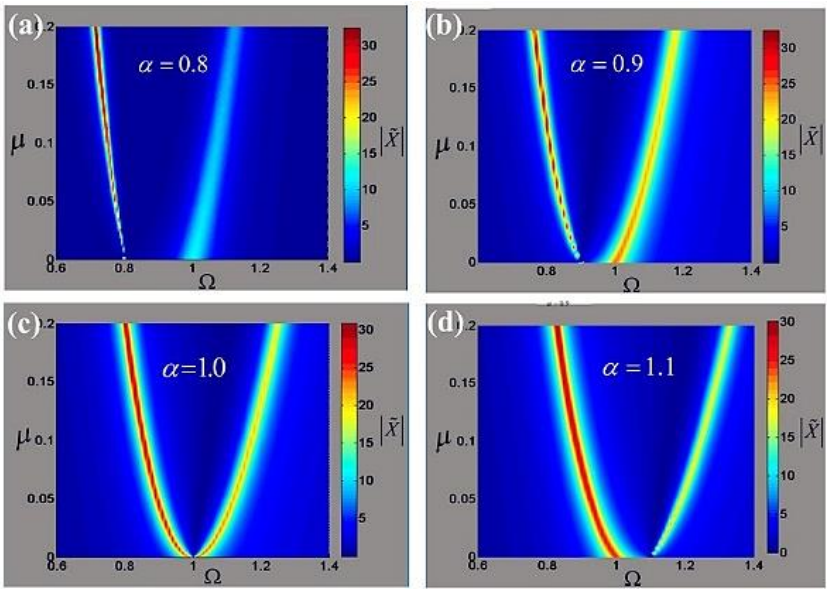

Figure 4. *Contour plotting of normalized displacement of the primary mass versus different mass ratios (μ) and frequency tuning ratios (α) under various excitation frequencies (Ω): (a) α=0.8; (b) α=0.9; (c) α=1.0; (d) α=1.1*

Table 1. *Design parameters of proposed 2DOF Piezoelectric MEMS energy harvesting chip*

Component	Designed parameter	Values
Primary mass	Height h_1	500 μm
	Radius R_1	1 mm
	Weight m_1	3.66 mg
Auxiliary mass	Outer radius R_3	5.4 mm
	Inner radius R_2	2.05 mm
	Weight m_2	91.3 mg
	Height h_2	500 μm
Outer spring beam	Height h_o	45 μm
	Circular arc angle θ	6.3°
	Inner radius R_4	5.5 mm
	Outer radius R_5	5.75 mm
Inner spring beam	Height h_i	45 μm
	Width w_i	200 μm
	Spacing l_i	50 μm
ZnO thin films	ZnO Thickness d_z	1.1μm
	Top Pt/Au d_t	300 nm
	Bottom Pt/Au d_t	300 μm
	Resistance R_i	240 kΩ
MEMS p-VEH chip	Volume V_o	14.5×14.5×0.5 mm^3

4. Results and Discussion

4.1 MEMS Device Characterization

Figure 5(a) shows optical image of the fabricated 2DOF MEMS piezoelectric energy harvesting chip. The overall size of the energy-harvesting chip is 14.5 mm×14.5 mm×500 μm. It is noted that the surface colour of the inner spiral beam and small circular mass become purple after micromachining process. This is probably due to the heat concentration problem during long-term DRIE process. SEM image of the inner auxiliary circular mass with parallel spiral beam is shown in Figure 5(b). It can be seen that the surface of beam and mass is kept approximately flat even though the thickness of the spiral beam is as thin as 43～45 μm. The top view of the top electrode/ZnO/bottom electrode sandwiched layers is shown in Figure 5(c). The multilayer structure is fabricated through a laminated layer-by-layer surface micromachining process. One of the key concerns is the short circuit problem of the top and bottom electrode. Therefore, during the ZnO thin film deposited by RF magnetron sputtering process, the bottom electrode should be fully covered by the ZnO semiconducting films. As shown in Figure 5(d), the line width of the top electrode is designed to be relatively narrow. Even though some misalignment may occur during multilayer deposition process, the overall device is still safe to operate normally.

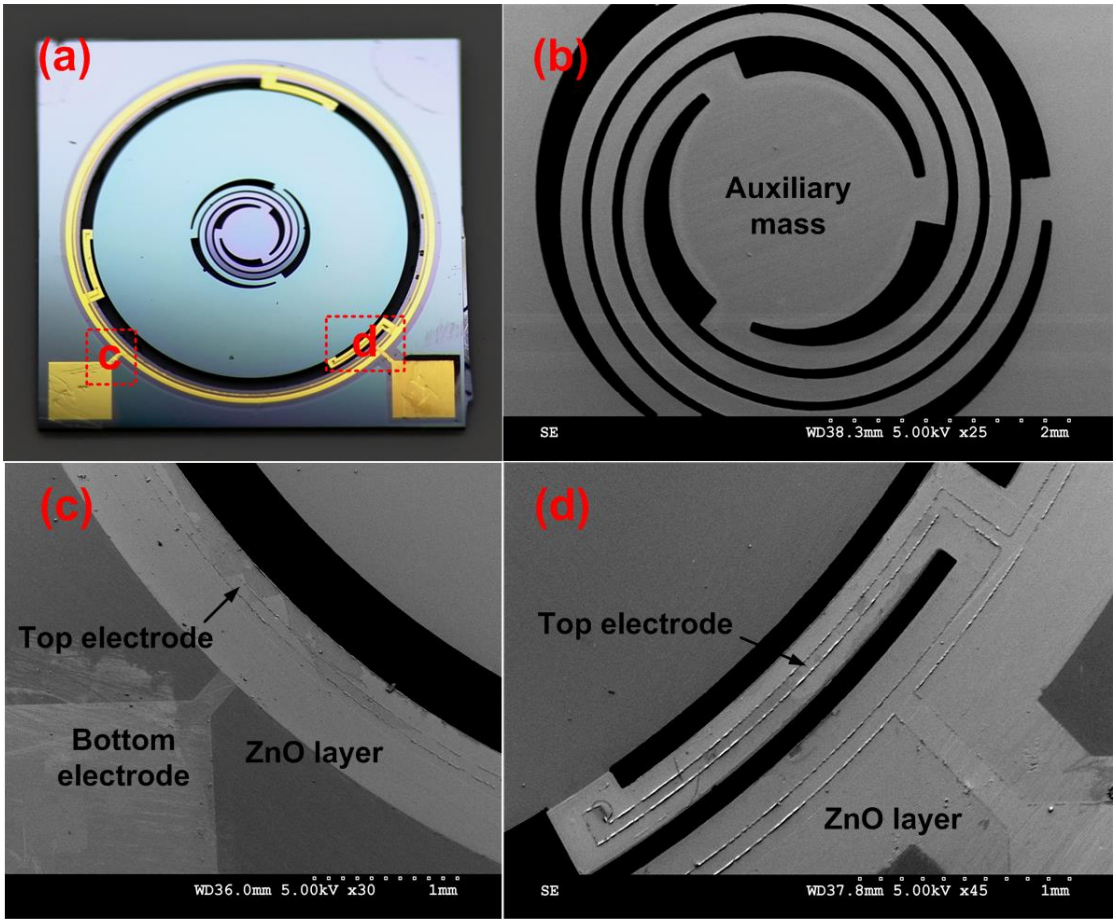

Figure 5. *(a) ZnO-based 2DOF piezoelectric energy harvesting chip; (b) SEM images of the auxilliary mass with inner spiral beams; (c) top view of ZnO thin film with top electrode; (d) SEM images of the outer circular-spring beam with ZnO thin film and top electrode*

The cross section of ZnO-based multilayer thin film is further characterized by field-emission scanning electron microscopy (FE-SEM), as shown in the Figure 6(a). The multilayered thin film structure can be clearly observed, including silicon substrate, SiO_2 insulation layer, bottom Pt/Au electrode layer, ZnO piezoelectric thin film layer and top Pt/Au electrode layer. The enlarged view of ZnO thin film is further characterized in Figure 6(b). The thickness of the ZnO and SiO_2 are around 1.1 and 0.5 μm, respectively. The cross sectional morphology clearly demonstrates that the ZnO thin film has uniform columnar texture which is grew perpendicularly to the top surface. This indicates that the ZnO thin film is highly c-axis-oriented and has excellent piezoelectric quality. The atom composition ratio of the multilayered structure is determined by energy dispersive X-ray spectroscopy spectrum analysis (EDS), as shown in Figure 6(c). The EDS analysis results demonstrate that the atomic percentages of oxygen, silicon, zinc and platinum are 53.98, 26.48, 17.91 and 18.37 %, respectively. These further confirms that silicon oxide insulation layer, zinc oxide piezoelectric layer and platinum conducting layer exist in the fabricated sample structure.

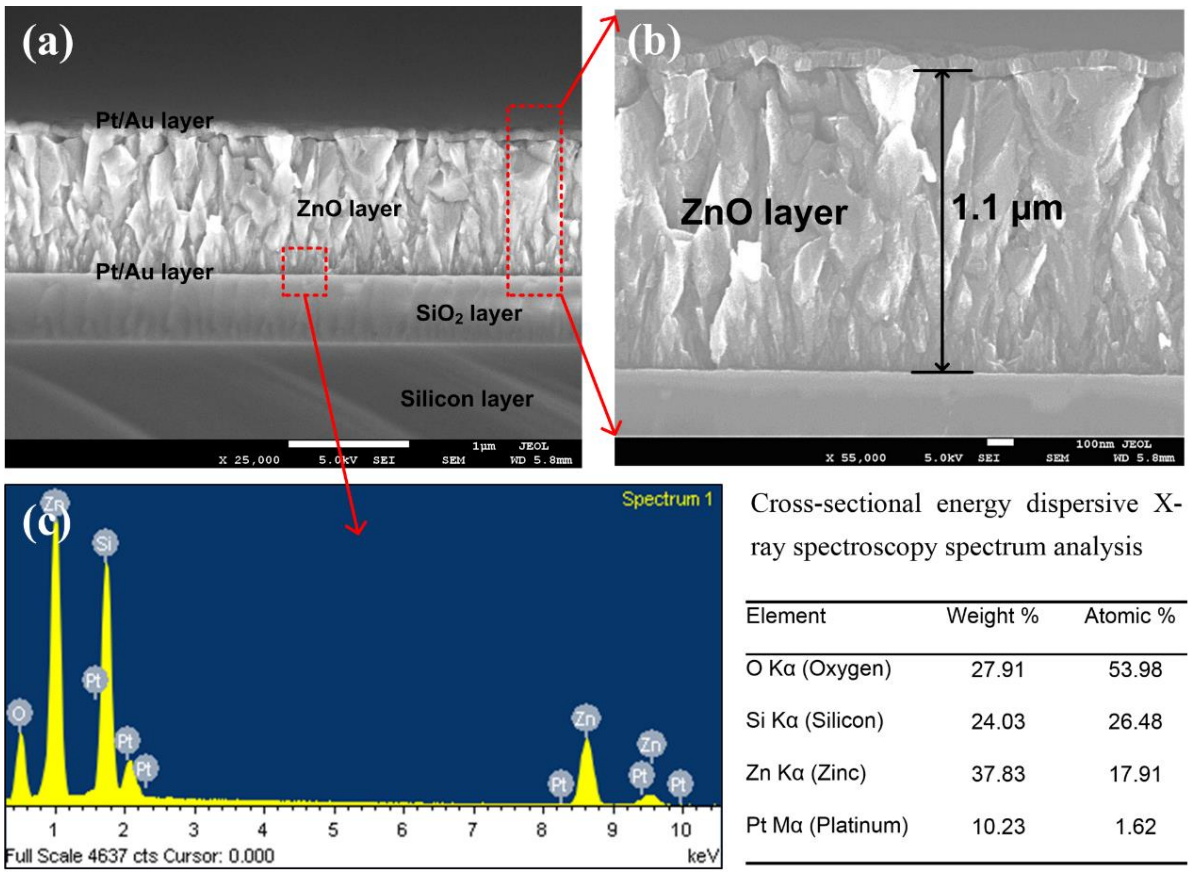

Cross-sectional energy dispersive X-ray spectroscopy spectrum analysis

Element	Weight %	Atomic %
O Kα (Oxygen)	27.91	53.98
Si Kα (Silicon)	24.03	26.48
Zn Kα (Zinc)	37.83	17.91
Pt Mα (Platinum)	10.23	1.62

Figure 6. *(a) Cross section of MEMS piezoelectric energy harvester with multilayered structure: Pt/Au conducting layer, ZnO piezoelectric layer, SiO_2 insulating layer and silicon-supporting layer; (b) Enlarged FE-SEM image of 1.1 μm thick ZnO thin film; (c) Energy dispersive X-ray spectroscopy spectrum analysis (EDS) of the piezoelectric multilayered structure*

4.2. Power Generation Experiments

The fabricated energy harvesting chip is further attached to a vibration testing system for electrical performance evaluation. The testing setup is mainly composed of a function generator, a voltage amplifier, an accelerometer, a shaker and a data acquisition system (DAQ NI USB-6289 M series). In the experiment, a swept frequency from 350 to 500 Hz at 0.5g and load resistance of 250 kΩ is applied to the MEMS 2DOF piezoelectric energy harvesting chip. Output voltage response in time-domain signal is directly recorded with DAQ sytem, as shown in Figure 7(a). It can been clearly seen that two comparable peak have been obtained with the output voltages around 10 and 15 mV, respectively. These are in good agreement with the previous modeling predications that two effective peaks can be readily obtained when the frequency tuning ratio α is around 0.9～1 and a small mass ratio near 0. By applying fast Fourier transform (FFT) to the time-domain signal, the frequency domain response can be derived, as shown in Figure 7(b). The resonant frequencies of the two peaks are found to be 403.8 and 489.9 Hz, respectively. The frequency ratio of the second peak to the first one is calculated to be only 1.21, exhibiting closer peaks compared to the previous studies in the literature [20, 21]. The output power and voltage of proposed 2DOF p-VEH device at various load resistances are presented in Figure 8. The operating frequency and excitation acceleration are set at 490 Hz and 0.5 g, respectively. The maximum output power is found to be 0.46 nW with an optimum load resistance of 240 kΩ. The normalized power

density of the p-VEH device, defined by power/volume/acceleration^2, is calculated as 1.75×10^{-7} W•cm^{-3}•g^{-2} for the particular device. Although the output power and power density of the present MEMS chip seems to be moderate at the current stage, it offers new insights in realizing complex piezoelectric MEMS harvesters with piezoelectric ZnO thin films.

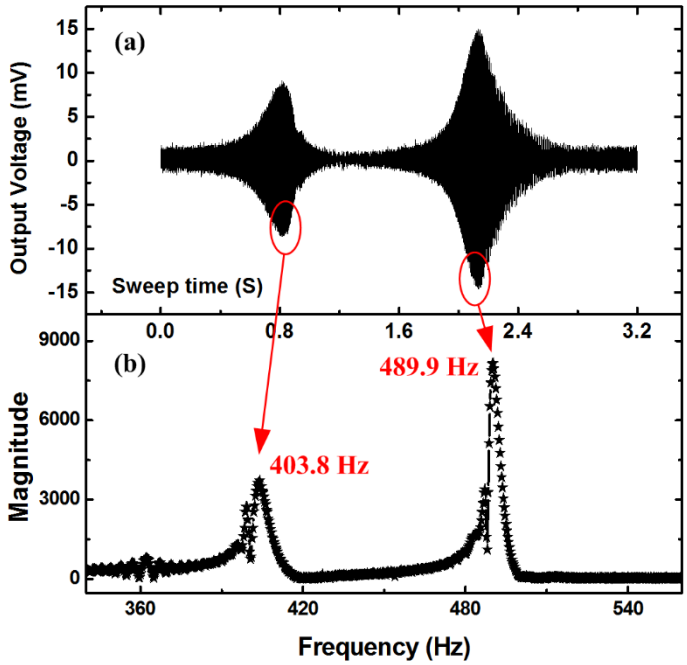

Figure 7. *Output voltage of the MEMS 2DOF piezoelectric energy harvester prototype with a swept frequency from 350 to 500 Hz: (a) output voltage in time domain response; (b) frequency domain signal by fast Fourier transform*

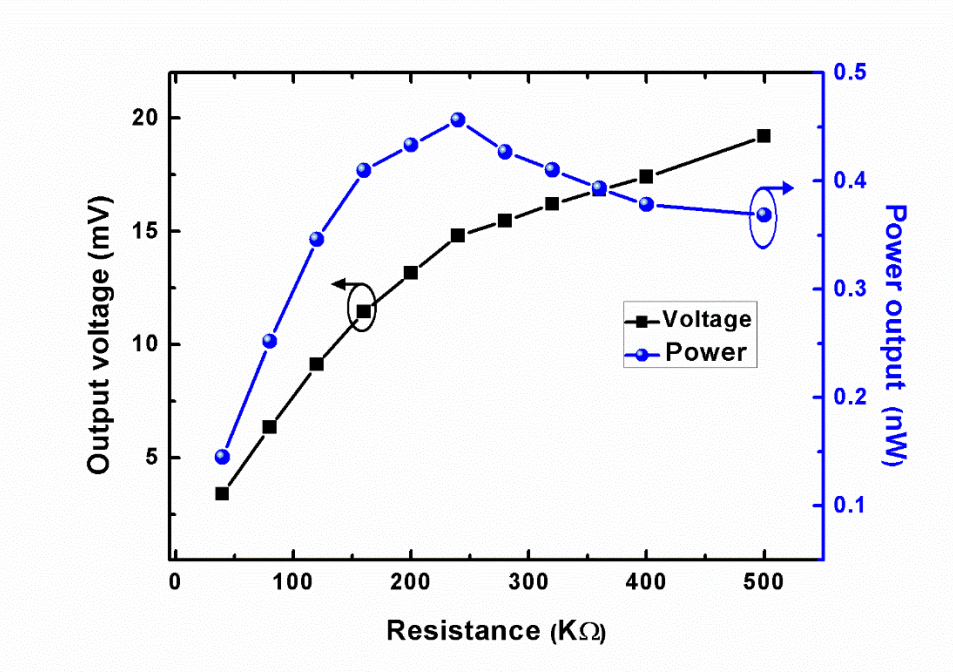

Figure 8. *Output voltage and power against different resistances at the resonance of 490 Hz with the acceleration of 0.5g*

5. Conclusion

In this paper, a fully integrated MEMS 2DOF energy harvester based on ZnO thin films has been successfully designed, modeled, fabricated and characterized. The MEMS p-VEH chip with volume of 14.5×14.5×0.5 mm^3 has a primary subsystem for energy conversion and an auxiliary subsystem for frequency adjustment. Through lumped parametric numerical analysis, it is found by controlling the frequency tuning ratio (α) in 0.9～1 and mass ratio (μ) approximate to 0, two close and comparable peaks can be obtained. The MEMS p-VEH chip is then successfully fabricated through a laminated layer-by-layer surface micromachining process and double-side DRIE bulk micromachining process. Both the MEMS device structure and power generation capability have been carefully characterized. Through FE-SEM and EDS analysis, it is found ZnO thin film is highly c-axis-oriented and has excellent piezoelectric quality. The power generation experiment demonstrates that close peaks of 403.8 and 489.9 Hz with comparable voltages of 10 and 15 mV are obtained respectively, providing good agreement with the modeling predictions. Although the performance of the current prototype is moderate, it offers new insights in realizing 2DOF multimode MEMS energy harvesting chip with piezoelectric ZnO thin films.

Acknowledgements

This research is supported by National Natural Science Foundation of China Grant No. 51705429, National Natural Science Foundation of Shaanxi Province No. 2018JQ5030 and the Fundamental Research Funds for the Central Universities No. 31020170QD070.

Reference

[1] P. Fang, X. Ma, X. Li, X. Qiu, R. Gerhard, X. Zhang, *et al.* Fabrication, structure characterization, and performance testing of piezoelectret-film sensors for recording body motion, *IEEE Sens. J.* 18(2018) 401-412.

[2] Y. Liao and J. Liang, Maximum power, optimal load, and impedance analysis of piezoelectric vibration energy harvesters, *Smart Mater. Struct.* 27(2018) 075053.

[3] Y. Yang, Y. Li, Y. Guo, B.-X. Xu, and T. Yang, Improved vibration-based energy harvesting by annular mass configuration of piezoelectric circular diaphragms, *Smart Mater. Struct.* 27(2018) 035004.

[4] K. Tao, J. Wu, A.G.P. Kottapalli, *et al.* Micro-patterning of resin-bonded NdFeB magnet for a fully integrated electromagnetic actuator, *Solid-State Electron.* 138(2017) 66-72.

[5] M. Halim, R. Rantz, Q. Zhang, L. Gu, K. Yang, and S. Roundy, An electromagnetic rotational energy harvester using sprung eccentric rotor, driven by pseudo-walking motion, *Appl. Energy,* 217(2018) 66-74.

[6] H. Liu, S. Gudla, F. A. Hassani, C. H. Heng, Y. Lian, and C. Lee, Investigation of the nonlinear electromagnetic energy harvesters from hand shaking, *IEEE Sens. J,* 15(2016) 2356-2364.

[7] Y. Zhang, T. Wang, A. Luo, Y. Hu, X. Li, and F. Wang, "Micro electrostatic energy harvester with both broad bandwidth and high normalized power density," *Appl. Energy,* 212(2018) 362-371.

[8] G. Chen, Y. Li, H. Xiao, and X. Zhu, "A micro-oscillation-driven energy harvester based on a flexible bipolar electret membrane with high output power," *J. of Mater. Chem. A,* 5(2017) 4150-4155.

[9] K. Tao, J. Wu, L. Tang, L. Hu, S. W. Lye, and J. Miao, Enhanced electrostatic vibrational energy harvesting using integrated opposite-charged electrets, *J. Micromech. Microeng.* 276(2017) 044002.

[10] Z. L. Wang, J. Chen, and L. Lin, "Progress in triboelectric nanogenerators as a new energy technology and self-powered sensors," *Energ. Environ. Sci.,* 8(2015) 2250-2282.
[11] P. Wang, R. Liu, W. Ding, *et al.* Complementary Electromagnetic‐Triboelectric Active Sensor for Detecting Multiple Mechanical Triggering, *Adv. Func. Mate.* 28 (2018) 1705808.
[12] H. Zhang, Y. Lu, A. Ghaffarinejad, and P. Basset, Progressive contact-separate triboelectric nanogenerator based on conductive polyurethane foam regulated with a bennet doubler conditioning circuit, *Nano Energy,* (51)2018 10-18.
[13] B. Yang, Y. Zhu, X. Wang, J.-q. Liu, X. Chen, and C. Yang, High performance PZT thick films based on bonding technique for d31 mode harvester with integrated proof mass, *Sens. and Actuators A: Physical*, 214(2014) 88-94.
[14] B. Norris, J. Anderson, J. Wager, and D. Keszler, "Spin-coated zinc oxide transparent transistors," *J. of Phys. D: Appl. Phys.,* (36)2003, 105
[15] V. L. Patil, S. A. Vanalakar, P. S. Patil, and J. H. Kim, "Fabrication of nanostructured ZnO thin films based NO2 gas sensor via SILAR technique," *Sens. and Actuators B: Physical*, 239(2017) 1185-1193.
[16] P. Wang, H. Du, S. Shen, M. Zhang, and B. Liu, Deposition, characterization and optimization of zinc oxide thin film for piezoelectric cantilevers, *Appl. Surf. Sci.,* (258)2012 9510-9517.
[17] Y. Fu, ZnO thin films and nanostructures for acoustic wave-based microfluidic and sensing applications, *Funct. Mate. Electron.*: *Apple Academic Press*, (262)2018 195-262.
[18] Y. Yuan, H. Du, K. S. Chow, M. Zhang, S. Yu, and B. Liu, Performance analysis of an integrated piezoelectric ZnO sensor for detection of head–disk contact, *Microsys. tech.,* (19)2013 1449-1455.
[19] L. Tang, Y. Yang, and C. Soh, Broadband Vibration Energy Harvesting Techniques, in *Advances in Energy Harvesting Methods*, Springer New York, 2013 17-61.
[20] Y. Tadesse, Shujun Zhang, and S. Priya, Multimodal Energy Harvesting System: Piezoelectric and Electromagnetic, *J. Intell. Mater. Syst. and Struct.,* (20)2009 625-632.
[21] Q. Ou, X. Chen, S. Gutschmidt, A. Wood, N. Leigh, and A. F. Arrieta, "An experimentally validated double-mass piezoelectric cantilever model for broadband vibration–based energy harvesting, *J. Intell. Mater. Syst. and Struct.,* (23)2012 117-126.
[22] K. Tao, L. Tang, J. Wu, S.W. Lye, H. Chang, and J. Miao, Investigation of multimodal electret-based MEMS energy harvester with impact-induced nonlinearity, *J. Microelectromech. Syst.,* (27)2018 276-288.
[23] L.C. Zhao, H.X. Zou, G. Yan, W.M. Zhang, Z.K. Peng, and G. Meng, Arbitrary-directional broadband vibration energy harvesting using magnetically coupled flextensional transducers, *Smart Mater. Struct.* 27(2018) 095010.
[24] H. T. Li, W. Y. Qin, J. Zu, and Z. Yang, Modeling and experimental validation of a buckled compressive-mode piezoelectric energy harvester, *Nonlinear Dynam.,* (24)2018 1-20.
[25] S. Zhou and L. Zuo, Nonlinear dynamic analysis of asymmetric tristable energy harvesters for enhanced energy harvesting, *Commun. Nonlinear Sci.* (61)2018 271-284.
[26] W. Tang, L.B. Wang, Y.M. Ren, B. Bao, and J.J. Cao, Design and experimental analysis of self-sensing SSDNC technique for semi-active vibration control, *Smart Mater. Struct.* 27(2018) 085028.